Published article:

T. R. B. Kushal and M. S. Illindala, "A Decision Support Framework for Resilience-Oriented Cost-Effective Distributed Generation Expansion in Power Systems," *IEEE/IAS 56th Industrial and Commercial Power Systems Technical Conference (I&CPS)*, Las Vegas, NV, USA, 2020, pp. 1–8, doi: 10.1109/ICPS48389.2020.9176823.

A Decision Support Framework for Resilience-Oriented Cost-Effective Distributed Generation Expansion in Power Systems

Tazim Ridwan Billah Kushal
Student Member, IEEE
The Ohio State University
2015 Neil Ave, Dreese Lab 205
Columbus, OH 43210, USA
kushal.1@osu.edu

Mahesh S. Illindala
Senior Member, IEEE
The Ohio State University
2015 Neil Ave, Dreese Lab 205
Columbus, OH 43210, USA
millindala@ieee.org

***Abstract*—Resilience of electricity grids to rare but severely disruptive events, such as natural disasters, has emerged in recent years as the most important aspect in power system planning. This paper presents a novel approach to enhance the resilience of a system by leveraging the distributed nature of solar photovoltaic (PV) and battery energy storage system (BESS) resources. The proposed decision-making framework uses analytic hierarchy process (AHP) to evaluate different possible allocations of PV and BESS resources for multiple contingencies based on resilience enhancement and cost. A deterministic formulation ranks outage scenarios based on the impact on performance. The trade-off between cost and resilience is modeled via cost-effectiveness analysis (CEA) that indicates the preferability of each allocation plan. The main contribution of this paper is the development of an adaptable and computationally feasible decision support framework to determine cost-effective configurations of PV arrays and BESSs for mitigating the effects of transmission line outage contingencies. To evaluate the proposed framework, a case study is carried out on the IEEE 33-bus radial distribution system. The results show that the proposed method can offer effective guidance to the planner for making informed decisions about spending resources and achieving cost-effective resilience enhancement.**

***Index Terms*—Decision support systems, distributed generation, power system planning, resilience, renewable energy**

I. Introduction

Traditional electric power systems are designed to operate during certain contingencies based on the reliability criteria of security and adequacy. These contingencies result from the breakdown of system components and have predictable impacts with known failure rates. However, catastrophic events such as natural disasters, which occur rarely but have a large and unpredictable impact, present a challenge to this reliability-based planning of power systems. Weather-related events can cause massive disruption of the grid in the form of infrastructure damage and service interruption. Hurricane Harvey was estimated to have caused $125 billion in total damages and power outage to about 220,000 customers [1]. In the period 2003-2012, over 50,000 U.S. customers were impacted by 679 power outages due to weather-related events [2]. Such high-impact and unpredictable contingencies require a resilience-oriented approach, since they cannot be addressed through the stochastic methods traditionally used in reliability-oriented planning.

Resilience is a concept distinct from reliability and indicates the ability of a system to deal with low-frequency high-impact events, which cannot be captured by reliability metrics [3]. Current practices with regard to distribution restoration leave the grid vulnerable to extreme weather events and are therefore not considered sufficiently resilient [4]. Probabilistic fragility modeling by Panteli et al. has shown that adaptation measures are necessary to ensure power system operation during extreme weather, particularly when key parameters such as wind speed are uncertain [5]. A study of the hazardous effects of wind storms in the Northeast U.S. using Sequential Monte Carlo simulations indicated the vulnerability of the grid to outage and the need for system hardening against wind storms [6]. Although similar probabilistic methods have been used to ensure reliable power system operation [7] and planning [8], they cannot guarantee mitigation against rare extreme events. Therefore, additional resilience-oriented alternatives have been explored in the literature.

Researchers have proposed various methods of enhancing the resilience of power systems [9]–[14]. One approach is to divide the grid into a number of smaller grids (islands) according to some grouping criteria to minimize load shedding and facilitate load restoration [9], [10]. A hierarchical outage management scheme has been used to design a resilient power distribution system encompassing multiple microgrids with distributed control [11]. The feeder restoration approach presented in [12] uses distributed energy resources (DERs) to supply the critical loads in a power distribution system when the main grid supply is unavailable. Replacing sections of a power system with underground natural gas transportation systems has been shown to improve the grid resilience [13]. In [14], a shipboard power system was made more resilient using a strategy of adding power lines based on graph theory.

Recent research has focused on exploiting the potential of locally available generation by using DERs to improve the

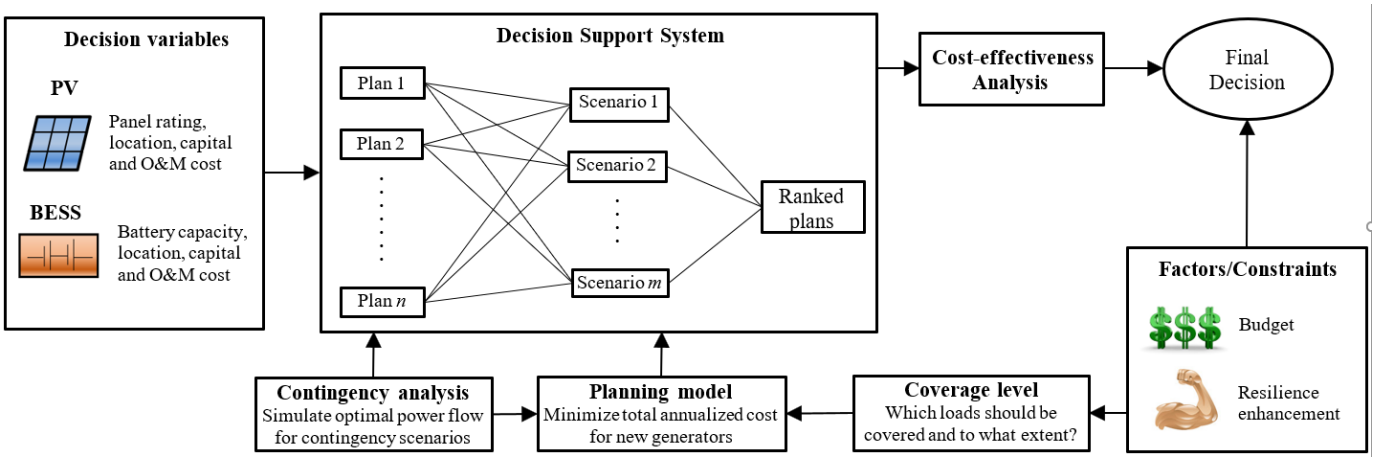

Fig. 1. Overview of the decision support framework.

resilience of the electric grid, especially on the distribution side, which has been shown by past experience as the most vulnerable part of the infrastructure [15]. The authors of [15] mention solar photovoltaic (PV) devices as one the potential DERs. Several methods of optimally sizing PV systems have been proposed [16]–[20]. Additionally, PV arrays are coupled with energy storage such as battery energy storage system (BESS) to resolve the problem of intermittent power output [21] and control power injection rate for system stability [22]. Their optimal sizing is generally treated as an optimization problem with a trade-off between cost and system reliability. Multi-objective approaches can include environmental considerations such as reduction of emissions (greenhouse gases and air pollutants) and fuel savings, either directly by maximizing the use of zero-emission sources [20] or indirectly (in grid-connected scenarios) by minimizing power purchases from the utility grid [18].

Literature concerning the planning of power systems based on PV and other renewable sources has generally focused on minimizing cost and ensuring reliability. Resilience has not been considered as an issue of interest. However, many of the outages reported in [1], [2] result from damaged transmission lines, which are crucial for the operation of conventional power systems with large generation capacities aggregated at a limited number of nodes. Renewable power generators tend to be distributed throughout the system and require fewer transmission lines [23], thus reducing the number of potential points of failure. Also, previous works have modeled multiple outage scenarios using probalistic methods. For example, Monte Carlo simulation is applied to model random outages in [8]. As discussed previously, this approach is unsuitable for resilience-oriented planning where the impact of outages is large and probability of occurrence is unknown. This paper aims to enhance the resilience of a power grid by exploiting the distributed nature of PV systems, which have greater sizing and siting flexibility than fossil fuel plants, along with BESSs to resolve the intermittency issue. Since adding more units would increase the resilience but would also cost more, cost-effectiveness analysis (CEA) is used to measure the performance per dollar spent. The major contribution of this paper is a flexible and scalable decision support system for PV system sizing and siting, shown in Fig. 1, that leverages its distributed nature to achieve higher resilience in a power distribution system. A deterministic formulation based on the severity of contingencies is used to model multiple outage scenarios simultaneously in the decision process.

The proposed framework in Fig. 1 is organized into the following sections. Section II describes the methodology of contingency analysis, ranking allocation plans and the decision support tool. Section III explains the planning model, where PV and BESS resources are optimally allocated for each scenario. Case study of a radial power distribution system using the proposed framework is presented in Section IV. Section V concludes the paper.

II. Multi-contingency Planning

The ability of a power system to supply loads is impaired by a transmission line outage, which prevents power flow through a subset of lines. This can happen because of direct physical damage to the line or tripped circuit breakers due to overloading. Regardless of the reason, it often ultimately causes a supply shortfall that results in some unserved load. In this study, the amount of unserved load is used as the measure of system performance.

A. Contingency Analysis

At any time, the state of a power system can be determined by running a power flow model. If the loads are considered dispatchable, this can also show the unserved load. The minimum unserved load under any condition may be determined by solving the cost-minimizing optimal power flow (OPF) problem, with a large cost incurred for any loads shed. Security-constrained OPF (SCOPF) can be used to deal with known contingencies by planning optimal corrective actions after a disruptive event [24]. However, the SCOPF formulation becomes increasingly complex as the pre-specified set of

contingencies grows larger. The order of contingency k, which in this study is the number of disabled transmission lines, determines the number of scenarios. For a system with n branches, the number of possible contingencies with k lines disabled is $\binom{n}{k}$. The IEEE 33-bus test system has 32 branches (excluding the normally-open tie lines) and for k = 1, 2, 3 and 4 the number of scenarios is 32, 496, 4960 and 35960 respectively. Since the set of scenarios grows rapidly with the order of the contingency, it may not be computationally feasible to consider all the possible scenarios. Robust programming approaches circumvent this problem by only selecting the worst contingencies using, for instance, a bi-level max-min formulation [25]. But this method has the disadvantage of increasing the cost by considering the worst possible scenario. This paper simulates the operating condition of the power system using conic programming, which offers a convenient way to solve OPF for radial AC systems using convex optimization [26]. The full non-convex optimization problem is reduced to a second-order cone programming (SOCP) problem by relaxing some constraints and eliminating other sinusoidal ones. The AC OPF is run for various contingencies and the results are used in the decision process.

B. Analytic Hierarchy Process

The Analytic Hierarchy Process (AHP) is a numerical framework for complex multiple criteria decision making [27]. It is a flexible decision support tool that can account for both objective realities and subjective experience through pairwise comparison of criteria and alternative options. Relative importance of each criterion with respect to all other criteria is expressed numerically, so that a higher number corresponds to greater importance. Similarly, each option is also compared against all other options under consideration and the relative preference, with respect to each criterion, is expressed as a number. If the number of criteria considered in a decision process is m, then a $m \times m$ pairwise comparison matrix of criterion weights $\mathbf{A}$ can be defined so that the element a_{jk} expresses the importance of the j-th criterion relative to the k-th criterion. With n alternative options being considered, a $n \times n$ pairwise comparison matrix $B^{(i)}$ can be constructed such that the element $b_{jk}^{(i)}$ indicates how preferable the j-th option is to the k-th option, with respect to the i-th criterion.

$$w_j = \frac{\sum_{k=1}^{m} \frac{a_{jk}}{\sum_{l=1}^{m} a_{lk}}}{m} \tag{1}$$

$$s_i^{(j)} = \frac{\sum_{k=1}^{n} \frac{b_{ik}^{(j)}}{\sum_{l=1}^{n} b_{lk}^{(j)}}}{n} \tag{2}$$

The pairwise comparison matrices are used to calculate the m-dimension criteria weight vector $\mathbf{w}$ and the n-dimensional option score vector $\mathbf{s}^j$ by normalization with the column sum and taking the row average, as shown in (1)–(2). The full $n \times m$ option score matrix is $\mathbf{S} = [\mathbf{s}^{(1)}\mathbf{s}^{(2)}...\mathbf{s}^{(m)}]$. As the final output, the AHP method assigns each option an overall score. The global score vector $\mathbf{v}$ gives the score for each option and is calculated as shown below.

$$\mathbf{v} = \mathbf{S}\mathbf{w} \tag{3}$$

The score of an option is a number that indicates its preferability. All n options can be arranged from most desirable to least desirable by arranging them in descending order of scores. In planning generation expansion for multiple contingencies, there is the issue of deciding the best plan for all possible scenarios. In this study, AHP has been used to solve this problem, by considering the contingencies as criteria and the plans as options. Criteria weights are assigned based on the severity of the contingencies, as indicated by the unserved load. Option scores are decided based on the performance of the plans in each scenario, evaluated on the basis of the power supplied and the annual cost. Cost-effectiveness of one option relative to another is calculated using the CEA metric of incremental cost effectiveness ratio (ICER). Since a lower ICER mean higher preferability, the utility score is defined as the inverse of ICER.

$$u_i(j,k) = \frac{E_j^{(i)} - E_k^{(i)}}{C_j - C_k} \tag{4}$$

$$U_k = \sum_i \sum_j u_i(j,k) \tag{5}$$

$$CE_j^{(i)} = \frac{C_j}{E_j^{(i)} - E_o^{(i)}} \tag{6}$$

In (4), the utility of the j-th plan compared to the k-th plan for the i-th contingency is denoted by $u_i(j,k)$. $E_j^{(i)}$ and $E_k^{(i)}$ are the effects of the j-th and k-th plans, respectively, when they are applied to the i-th contingency, defined as the amount of load supplied. C_j and C_k are the annualized investment cost plus the annual operating cost of the j-th and k-th plans respectively. According to (4), a plan has higher utility if it supplies more power and has a lower annual cost, since a plan that can supply more power per additional dollar is considered to be more cost-effective. The total utility of the k-th plan U_k is calculated by summing over all the comparisons and contingencies as shown in (5). The average cost-effectiveness ratio for the j-th plan in the i-th contingency $CE_j^{(i)}$ is calculated as shown in (6), where $E_o^{(i)}$ is the active power supplied in that scenario without any additional generators. The utility function is used to build the pairwise comparison matrices for the AHP algorithm using the transformations shown below.

$$x_{jk} = 1 + 8\left(\frac{\frac{1}{P_j^{US}} - \frac{1}{P_k^{US}}}{\max P^{US} - \min P^{US}}\right) \tag{7}$$

$$a_{jk} = \begin{cases} x_{jk} & : x_{jk} \geq 1 \\ \frac{1}{x_{jk}} & : x_{jk} < 1 \\ 1 & : otherwise \end{cases} \tag{8}$$

$$y_{jk}^{(i)} = 1 + 8\left(\frac{\sum_l u_i(l,j) - \sum_l u_i(l,k)}{u_{max}^{(i)} - u_{min}^{(i)}}\right) \tag{9}$$

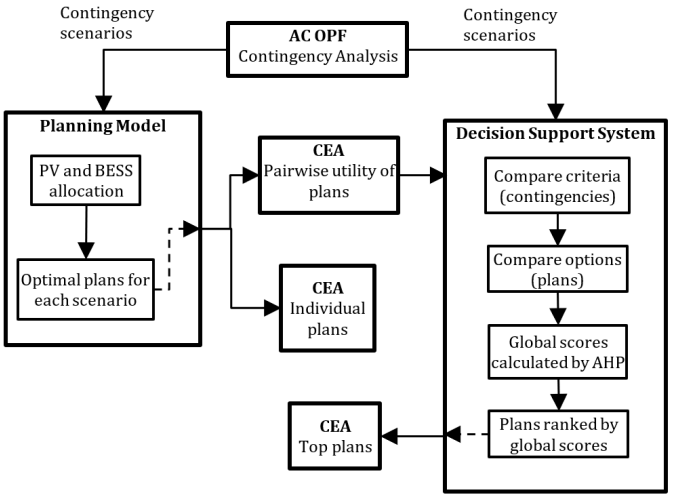

Fig. 2. Proposed planning framework for resilience enhancement.

$$b_{jk}^{(i)} = \begin{cases} y_{jk}^{(i)} & : y_{jk}^{(i)} \geq 1 \\ \frac{1}{y_{jk}^{(i)}} & : y_{jk}^{(i)} < 1 \\ 1 & : otherwise \end{cases} \tag{10}$$

Contingencies are compared on the basis of severity, which is represented by the amount of unserved load. P_j^{US} and P_k^{US} are the total unserved load in the k-th and j-th contingencies, respectively. Therefore, criteria are assigned importance by (7)–(8), where $\max P^{US}$ and $\min P^{US}$ are the maximum and minimum unserved load across all contingencies, respectively. Similarly, option scores are calculated in (9)–(10), with $u_{max}^{(i)}$ and $u_{max}^{(i)}$ denoting the maximum and minimum utility among all plans for contingency i, respectively. A simple linear transformation is used to derive the matrices in each case. Results of the contingency simulation are used as the basis for the planning model and decision support system, as shown in Fig. 2.

III. Allocation and Sizing of PV and BESS

Transmission line outages reduce the number of available paths for power flow and may cause a shortfall in supply. Appropriately sized solar PV arrays, along with a BESS as a backup source and storage for excess energy, can supply the shortfall. The node with the highest unserved load across all the contingencies is selected for these resources. A disabled transmission line divides the grid into islands, which are groups of nodes with an existing path between each pair of nodes. Based on the results of AC OPF simulation described in Section II, the planning model allocates PV and BESS resources to each island to ensure that the demand is met at minimum cost. Fig. 2 how the optimal plan for each scenario is used to calculate cost-effectiveness and provide input to the AHP algorithm.

A. Photovoltaic Resources

A PV array equipped with a dc-ac inverter and a maximum power point tracking (MPPT) controller has a power output

TABLE I
PV panel parameters

PV panel	BP-Solar 3200
Rated power	200 W
Open-circuit voltage	30.8 V
Short-circuit current	8.7 A
Optimum voltage	24.5 V
Optimum current	8.16 A
Efficiency at STC	13%
Dimensions (L/W/D)	1680 × 837 × 50 mm
Cost per panel	$420
O&M cost	$15/kW

TABLE II
Lead-acid battery parameters

Battery	Hoppecke 6OPzS 600
Rated capacity	600 Ah
Rated voltage	2 V
Minimum SOC	35%
Round-tip efficiency	85%
Max. charge/discharge rate	0.5 A/Ah, 0.5 A/Ah
Max. charge/discharge current	100 A/75 A
Self-discharge rate	1%
Dimensions (L/W/D)	215 × 193 × 710 mm
Cost per cell	$150
O&M cost	$20/kAh

the depends on the solar irradiance and temperature. The PV array installed for island i is rated at $P_{pv\_r}^{(i)}$ with a derating factor of $f_{pv}^{(i)}$ to account for various factors such as shading and wiring losses. The actual power output of the array $P_{pv}^{(i)}$ depends on the on the solar insolation G and the temperature T. The solar radiation and temperature under standard test conditions are given by G_{STC} and T_{STC} respectively, while α_T is the temperature coefficient.

$$P_{pv}^{(i)} = f_{pv}^{(i)} P_{pv\_r}^{(i)} \frac{G}{G_{STC}} [1 + \alpha_T (T - T_{STC})] \tag{11}$$

$$f(G; a, b) = \frac{\Gamma(a+b)}{\Gamma(a)\Gamma(b)} \left(\frac{G}{G_{max}}\right)^{a-1} \left(1 - \frac{G}{G_{max}}\right)^{b-1} \tag{12}$$

$$P_{pv\_r}^{(i)} = n_{pv}^{(i)} P_{pv\_unit} \tag{13}$$

The expression in (11) gives the instantaneous PV power output for a given solar radiation and temperature. Since solar irradiance changes with time, the output power also varies, so a stochastic model is needed to account for the time-varying nature and suggest an appropriate value for G. As in many previous studies, the insolation is assumed to follow a beta probability distribution function [28] given by (12), where a and b are the shape parameters of the beta distribution and γ is the gamma function. Therefore, the allocated PV resources would have to be oversized in order to supply the demand. In (13), PV installation for island i is shown to be made up of $n_{pv}^{(i)}$ discrete units, each with rated power P_{pv_unit} . The full list of PV panel parameters is provided in Table I.

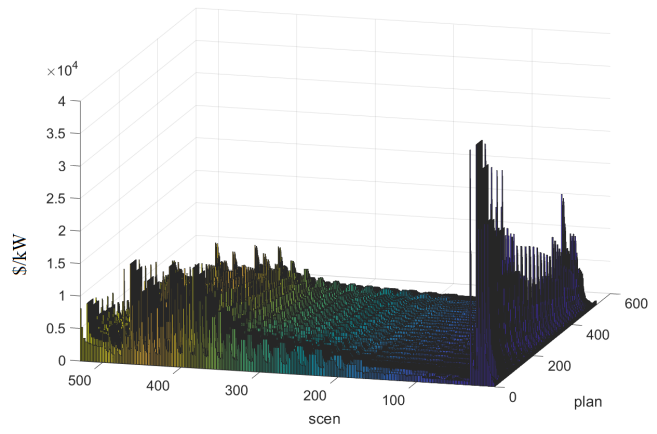

Fig. 3. Cost-effectiveness for all plans and scenarios.

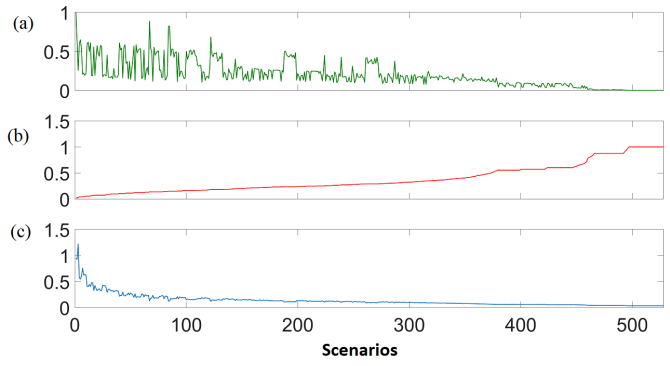

Fig. 4. Relationship between normalized (a) total unserved load, (b) cost, and (c) utility score.

B. Lead-Acid Battery

Since PV arrays alone cannot reliably supply power, some form of energy storage is needed to match supply with demand. Usually, lead-acid batteries are combined with PV arrays for this purpose. The battery can be charged during periods of surplus production and discharged when there is a deficit, so that the loads are always supplied. Allocation of batteries to each island is described by

$$Q_{bs}^{(i)} = n_{bs}^{(i)} Q_{bs\_unit} \tag{14}$$

where $Q_{bs}^{(i)}$ is the ampere-hour capacity of the BESS installed in island i, $n_{bs}^{(i)}$ is the number of cells in the battery, and Q_{bs_unit} is the rated ampere-hour capacity of each cell. The ampere-hour charge is used here since for batteries it is more convenient than energy or power. The BESS also includes an inverter and charge controller. The maximum depth of discharge and the efficiencies of the inverter and controller are considered in the model. Since PV arrays provide no power during the night, a robust sizing strategy is used to decide the BESS capacity so that it can take on the entire unserved load by itself. Table II gives the details of the lead-acid battery cells used.

C. Annual Cost

The purpose of the planning model is the optimal sizing and allocation of the resources to enhance resilience and minimize total cost. This is formulated as an optimization problem with the total annual cost as the objective function and the various requirements enforced as constraints.

$$\min_{n_{pv}^{(i)}, n_{bs}^{(i)}} f_{cr} \left(C_{pv} \sum_i n_{pv}^{(i)} + C_{bs} \sum_i n_{bs}^{(i)} \right) + C_{pv\_OM} \sum_i P_{pv\_r}^{(i)} + C_{bs\_OM} \sum_i Q_{bs}^{(i)} \tag{15}$$

$$f_{cr} = \frac{r(1+r)^L}{(1+r)^L - 1} \tag{16}$$

Total annualized cost is represented as expression in (15). The initial investment cost is found by multiplying the number of installed units by the cost per unit. C_{pv} and C_{bs} are the costs of each PV and BESS unit respectively, as specified in Tables I and II. The cost is annualized by multiplying it with the capital recovery factor f_{cr}, calculated as in (16), where r is the interest rate and L is the project lifetime. The annual operating and maintenance cost is calculated using the per unit capacity costs of PV and BESS, which are C_{pv_OM} and C_{bs_OM} respectively. Since resilience enhancement is the primary goal and normal operation is not a priority, fuel savings and tax credits are not included in the cost calculations, unlike in [20]. However, realistically a system planner would intend to use the PV generation and cheap electricity used to charge the BESS during off-peak hours to get added return on investment. These considerations would reduce the total annualized cost and provided a further incentive for generation expansion.

IV. Case Study

Radial power distribution systems are particularly vulnerable to line outages, since disruption of a single line may cut off multiple buses from power. The proposed planning method is tested on the standard IEEE 33-bus system, a 12.66 kV radial distribution system with total active and reactive power of 3.71 MW and 2.3 MVAR respectively [29]. Numerical solutions are obtained using CPLEX 12.8.0.0 optimization solver in MATLAB. All first- and second-order contingencies (one and two lines disabled, respectively) are simulated using the AC OPF model to yield the amount of unserved load at each node, considering all loads as dispatchable. The SOCP model is run for 528 contingencies. In the planning model, mixed-integer linear programming (MILP) is used to solve the optimization problem of minimizing total annual cost for each contingency scenario. The numerical solution to the MILP problem gives the optimal plans for all scenarios, which are used as options in the AHP decision-making stage.

A. Evaluation of Recommended Plans

The cost-effectiveness of each option for all scenarios is evaluated using (6) and the result is shown in Fig. 3. Plans are generally the least cost-effective for the first few

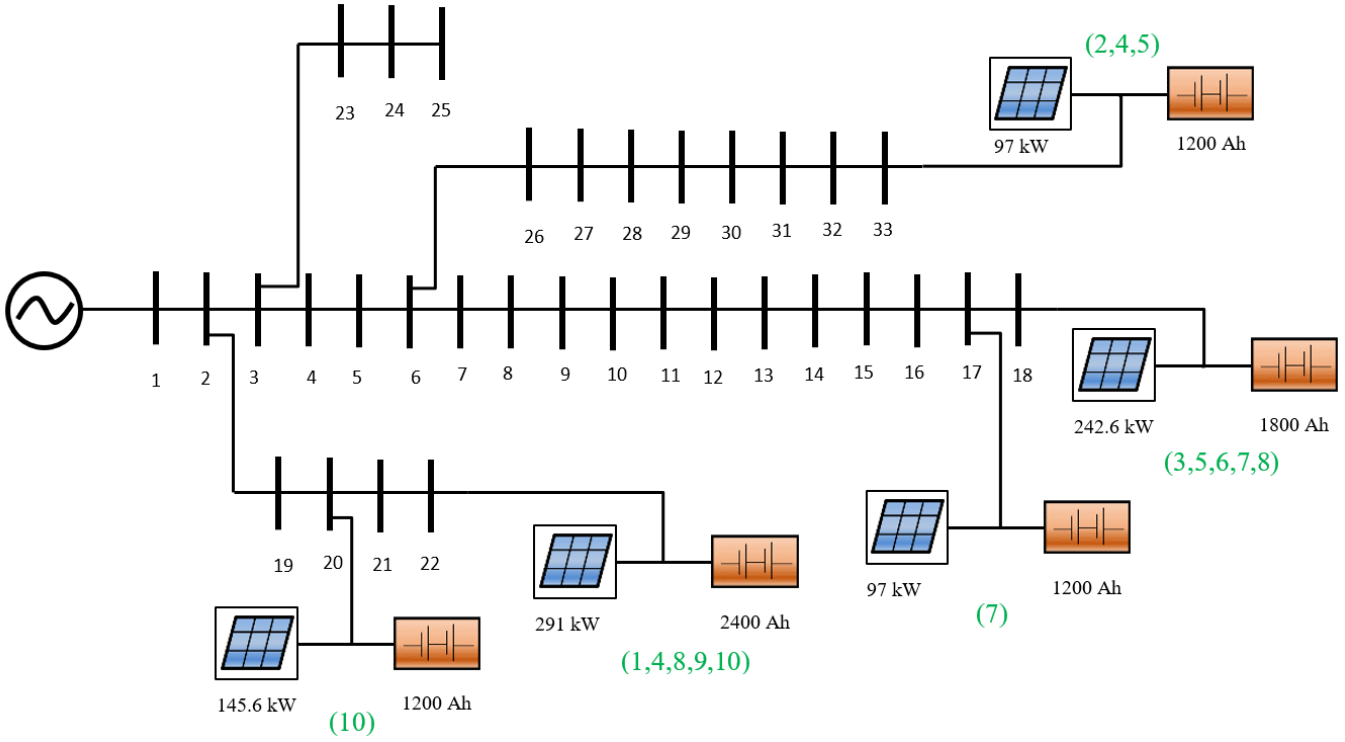

Fig. 5. The 33-bus distribution system with top 10 plans implemented, showing rated solar array power and battery capacity along with options.

scenarios, where most of the buses are disconnected from the only generator bus (bus 1). These are the scenarios with the highest load shedding and require the most expensive plans. Comparison of the options on the basis of unserved load, cost, and utility (normalized with respect to the maximum), demonstrated in Fig. 4, show that costlier plans supply more power but generally tend to be less cost-effective. This trend of diminishing returns means that the planner must consider the trade-off between performance and cost-effectiveness using the decision support system described in Section II. Since the utility score is based on the pairwise comparison of plans, Fig. 4 indicates that cheaper plans are generally preferable to expensive ones.

All options are ranked according to their AHP global scores based on the utility function in (4). The options are not mutually exclusive and often overlapping. For example, if Plan A requires a 728-cell solar array and Plan B requires a 1213-cell solar array at the same bus, then implementing Plan B is equivalent to combining the two. The planner may choose to combine multiple options while staying within budget. Fig. 5 shows the result of implementing the first 10 plans recommended by AHP. The PV and BESS units are added preferentially to terminal buses, which are more vulnerable to load shedding due to being further away from the generation bus.

B. Coverage Level

The results shown in Figs. 3-5 have assumed that the planner intends to cover all of the unserved load with additional

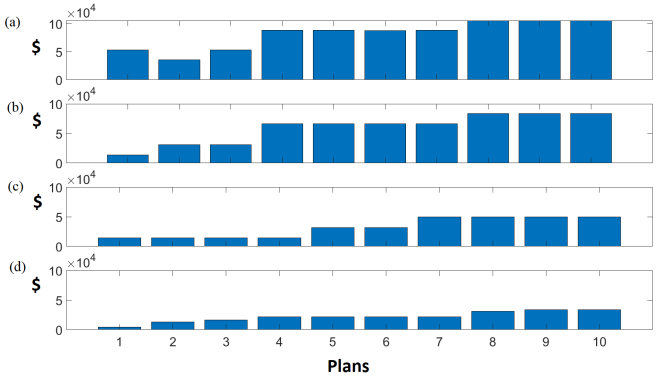

Fig. 6. Cost for the top 10 plans for (a) 100% (b) 99% (c) 95% and (d) 80% coverage.

generation. The effect of reducing the coverage of unserved load, which may be necessary due to priorities and budget constraints, is also investigated in this case study. For some contingency scenarios where the unserved load is too low, the annualized cost of the optimal plan becomes zero and these scenarios ignored in the AHP stage. Fig. 6 compares the cost of the top 10 plans for different levels of coverage. Fig. 7 does the same thing for total cost-effectiveness, defined as the sum of $CE_j^{(i)}$ for all contingencies i, revealing a pattern similar to Fig. 3. The results show a significant reduction in total cost and cost per unit power as the coverage level is reduced from 100% to 80%. This is the same trend seen in Fig. 3 of more expensive plans not only costing more in total but also being

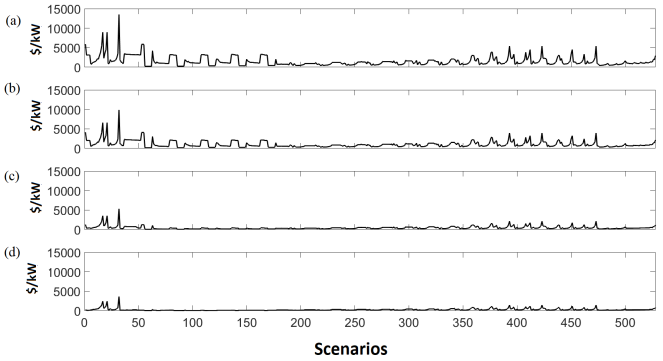

Fig. 7. Total cost-effectiveness for (a) 100% (b) 99% (c) 95% and (d) 80% coverage.

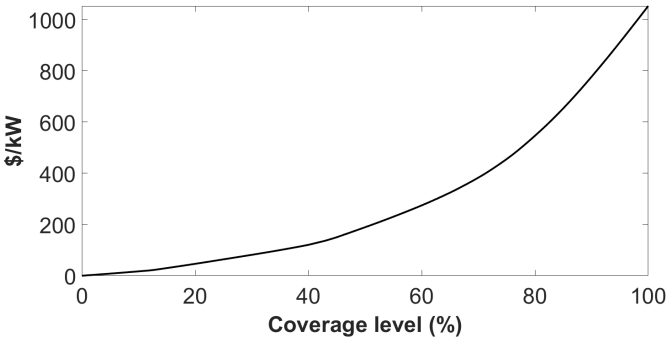

Fig. 8. Average cost-effectiveness for different levels of coverage, for 0% to 100%.

more expensive per kW. The average cost per kW of additional power capacity, calculated over all the plans and scenarios, is plotted for a broader range of coverage levels in Fig. 8. It shows that each unit of resilience enhancement becomes more expensive as larger proportions of loads are planned for. The results suggest that costs scale faster than a linear rate, which planners of large systems should be aware of. The coverage level is a matter of policy for the planner, as shown in Fig. 1. In this study, all the loads are assumed to be dispatchable and equally weighted. A more detailed model could include weighted loads or partitioning the set into vital and non-vital loads. This would make some loads more expensive to cover, based on not just size but also location.

V. Conclusion

This paper presents a flexible and generalizable decision-making framework to enhance the resilience of a power system against transmission line outages while making the best use of financial investment. Contingencies are simulated by an AC OPF model and the results are used as input for the planning stage, where PV and BESS resources are optimally allocated to ensure that all loads are supplied at minimum cost. Since multiple contingencies are being considered and several plans are possible, AHP is used as a decision support system to choose between the available alternatives, ranked according to their cost-effectiveness and performance in various contingency scenarios with varying severity. A case study conducted on the 33-bus radial distribution system demonstrates the effectiveness of the framework as a decision support tool. Analysis of the results shows that decision-makers can reduce the cost per unit power by choosing cheaper generation expansion plans and allowing some load shedding to occur.

The proposed method offers significant flexibility and transparency for decision-makers. In this study, cost and resilience have been considered as the determining factors for the utility of alternative plans, but any number of factors may be included. The utility function may be replaced by a different formula or an implicit system such as a learning algorithm. The set of scenarios may be expanded to include higher-order contingencies. Quantitative analysis reveals patterns that may help planners make a compromise between cost and resilience, perhaps through a secondary decision support system based on their own priorities. Since AHP only uses linear transformations, it may be scaled up to include more contingencies and allocation plans without requiring significantly greater computational power. The list of options in the case study of Section IV has been limited to the optimal plans for all scenarios, but the planning model may be expanded to generate any number of options. The framework developed in this paper helps decision-makers choose the best generation expansion strategy to limit cost and maximize resilience. This approach provides decision-makers with a tool for evaluating multiple contingency plans and building a resilient power system that can remain operational despite the occurrence of rare extreme events.

References

[1] E. S. Blake and D. A. Zelinsky, Tropical Cyclone Report: Hurricane Harvey (AL092017), Miami, FL, May 2018

[2] Y. Wang, C. Chen, J. Wang, and R. Baldick, "Research on Resilience of Power Systems under Natural Disasters - A Review," *IEEE Trans. Power Syst.*, vol. 31, no. 2. pp. 1604–1613, Mar. 2016.

[3] Z. Bie, Y. Lin, G. Li, and F. Li, "Battling the Extreme: A Study on the Power System Resilience," *Proc. IEEE*, vol. 105, no. 7, pp. 1253–1266, Jul. 2017.

[4] C. Chen, J. Wang, and D. Ton, "Modernizing Distribution System Restoration to Achieve Grid Resiliency Against Extreme Weather Events: An Integrated Solution," *Proc. IEEE*, vol. 105, no. 7, pp. 1267–1288, Jul. 2017.

[5] M. Panteli, C. Pickering, S. Wilkinson, R. Dawson, and P. Mancarella, "Power System Resilience to Extreme Weather: Fragility Modeling, Probabilistic Impact Assessment, and Adaptation Measures," *IEEE Trans. Power Syst.*, vol. 32, no. 5, pp. 3747–3757, Sep. 2017.

[6] G. Li et al., "Risk Analysis for Distribution Systems in the Northeast U.S. Under Wind Storms," *IEEE Trans. Power Syst.*, vol. 29, no. 2, pp. 889–898, Mar. 2014.

[7] L. Wu, M. Shahidehpour, and T. Li, "Stochastic security-constrained unit commitment," *IEEE Trans. Power Syst.*, vol. 22, no. 2, pp. 800–811, May 2007.

[8] A. Khodaei and M. Shahidehpour,"Microgrid-based co-optimization of generation and transmission planning in power systems," *IEEE Trans. Power Syst.*, vol. 28, no. 2, pp. 1582–1590, 2013.

[9] T. Amraee and H. Saberi, "Controlled islanding using transmission switching and load shedding for enhancing power grid resilience," *Int. J. Electr. Power Energy Syst.*, vol. 91, pp. 135–143, 2017.

[10] T. Ding, Y. Lin, Z. Bie, and C. Chen, "A resilient microgrid formation strategy for load restoration considering master-slave distributed generators and topology reconfiguration," *Appl. Energy*, vol. 199, pp. 205–216, 2017.

[11] H. Farzin, M. Fotuhi-Firuzabad, and M. Moeini-Aghtaie, "Enhancing Power System Resilience Through Hierarchical Outage Management in Multi-Microgrids," *IEEE Trans. Smart Grid*, vol. 7, no. 6, pp. 2869–2879, Nov. 2016.

[12] A. Dubey and S. Poudel, "A robust approach to restoring critical loads in a resilient power distribution system," in *IEEE Power and Energy Society General Meeting*, 2017, pp. 15.

[13] C. Shao, M. Shahidehpour, X. Wang, X. Wang, and B. Wang, "Integrated Planning of Electricity and Natural Gas Transportation Systems for Enhancing the Power Grid Resilience," *IEEE Trans. Power Syst.*, vol. 32, no. 6, pp. 4418–4429, Nov. 2017.

[14] K. Lai and M. S. Illindala, "Graph Theory Based Shipboard Power System Expansion Strategy for Enhanced Resilience," *IEEE Trans. Ind. Appl.*, vol. 54, no. 6, pp. 5691–5699, 2018.

[15] R. Arghandeh et al., "The Local Team: Leveraging Distributed Resources to Improve Resilience," *IEEE Power Energy Mag.*, vol. 12, no. 5, pp. 76–83, Sep. 2014.

[16] W. D. Kellogg, M. H. Nehrir, G. Venkataramanan, and V. Gerez, "Generation unit sizing and cost analysis for stand-alone wind, photovoltaic, and hybrid wind/PV systems," *IEEE Trans. Energy Convers.*, vol. 13, no. 1, pp. 70–75, Mar. 1998.

[17] W. Kellogg, M. H. Nehrir, G. Venkataramanan, and V. Gerez, "Optimal unit sizing for a hybrid wind/photovoltaic generating system," *Electr. Power Syst. Res.*, vol. 39, no. 1, pp. 35–38, Oct. 1996.

[18] R. Chedid and S. Rahman, "Unit sizing and control of hybrid wind-solar power systems," *IEEE Trans. Energy Convers.*, vol. 12, no. 1, pp. 79–85, Mar. 1997.

[19] Lin Xu, Xinbo Ruan, Chengxiong Mao, Buhan Zhang, and Yi Luo, "An Improved Optimal Sizing Method for Wind-Solar-Battery Hybrid Power System," *IEEE Trans. Sustain. Energy*, vol. 4, no. 3, pp. 774–785, Jul. 2013.

[20] C. Yuan, M. S. Illindala, and A. S. Khalsa, "Co-Optimization Scheme for Distributed Energy Resource Planning in Community Microgrids," *IEEE Trans. Sustain. Energy*, vol. 8, no. 4, pp. 1351–1360, Oct. 2017.

[21] P. Denholm and R. M. Margolis, ''Evaluating the limits of solar photovoltaics (PV) in electric power systems utilizing energy storage and other enabling technologies," *Energy Policy*, vol. 35, no. 9, pp. 4424–4433, Sep. 2007.

[22] D. Álvaro, R. Arranz, and J. A. Aguado, "Sizing and operation of hybrid energy storage systems to perform ramp-rate control in PV power plants," *Int. J. Electr. Power Energy Syst.*, vol. 107, pp. 589–596, 2019.

[23] R. Domínguez, A. J. Conejo, and M. Carrión, "Toward fully renewable electric energy systems," *IEEE Trans. Power Syst.*, vol. 30, no. 1, pp. 316–326, Jan. 2015.

[24] A. Monticelli, M. V. F. Pereira, and S. Granville, "Security-Constrained Optimal Power Flow with Post-Contingency Corrective Rescheduling," *IEEE Trans. Power Syst.*, vol. 2, no. 1, pp. 175–180, 1987.

[25] X. Wu, A. J. Conejo, and N. Amjady, "Robust security constrained ACOPF via conic programming: Identifying the worst contingencies" *IEEE Trans. Power Syst.*, vol. 33, no. 6, pp. 5884–5891, Nov. 2018.

[26] R. A. Jabr, "Radial Distribution Load Flow Using Conic Programming," *IEEE Trans. Power Syst.*, vol. 21, no. 3, pp. 1458–1459, Aug. 2006.

[27] T. L. Saaty, "How to make a decision: The analytic hierarchy process," *Eur. J. Oper. Res.*, vol. 48, no. 1, pp. 9–26, Sep. 1990.

[28] Y. M. Atwa, E. F. El-Saadany, M. M. A. Salama, and R. Seethapathy, "Optimal renewable resources mix for distribution system energy loss minimization," *IEEE Trans. Power Syst.*, vol. 25, no. 1, pp. 360–370, 2010.

[29] M. E. Baran and F. F. Wu, "Network reconfiguration in distribution systems for loss reduction and load balancing," *IEEE Trans. Power Deliv.*, vol. 4, no. 2, pp. 1401–1407, Apr. 1989.